Localized exciton-polariton modes in dye-doped nanospheres: a quantum approach

Martin J Gentile, Simon A R Horsley, William L Barnes

School of Physics and Astronomy, University of Exeter, Exeter EX4 4QL, UK

E-mail: m.j.gentile@exeter.ac.uk, s.horsley@exeter.ac.uk, w.l.barnes@exeter.ac.uk

Abstract. We model a dye-doped polymeric nanosphere as an ensemble of quantum emitters and use it to investigate the localized exciton-polaritons supported by such a nanosphere. By determining the time evolution of the density matrix of the collective system, we explore how an incident laser field may cause transient optical field enhancement close to the surface of such nanoparticles. Our results provide further evidence that excitonic materials can be used to good effect in nanophotonics.

PACS numbers: 7135Gg, 4250Ct, 7135Cc, 7722Ch, 4250Md

Keywords: Optical field enhancement, J-aggregate, Exciton, Permittivity, Nanophotonics, Density matrix

Submitted to: *J. Opt.*

1. Introduction

Plasmonic nanoparticles exhibit optical field enhancement when localized surface plasmon polariton (SPP) resonances are excited [1, 2]. The strength of the enhancement depends sensitively on the nanoparticle's environment and geometry [3]. The enhancement is a vital part of phenomena such as surface-enhanced Raman scattering [4], and finds application in areas such as biosensing [5], monitoring lipid membranes [6], modifying molecular fluorescence [7] and materials characterization [8]. Localized SPP resonances occur because of the way the free conduction electrons in metal particles respond to light. For many metals at optical frequencies their response is such that the permittivity is negative - a critical requirement if the nanoparticle is to support a plasmon mode.

However, metals are not the only materials to exhibit negative permittivity; materials doped with excitonic organic dye molecules are of interest for photonics [9] and may also possess negative permittivity over a small frequency range [10]. Interest in such materials as a means to support surface exciton-polariton (SEP) resonances has recently been rekindled [11, 12, 13]. An example of this class of material is a polymer doped with dye molecules. In a previous work we showed, through experiment and with the aid of a classical model, that polyvinyl alcohol (PVA) doped with TDBC molecules (*5,6-dichloro-2-[[5,6-dichloro-1-ethyl-3-(4-sulphobutyl)-benzimidazol-2-ylidene]-propenyl]-1-ethyl-3-(4-sulphobutyl)-benzimidazolium hydroxide*, sodium salt, inner salt) may support localized surface exciton-polariton modes. We extracted the complex permittivity $\varepsilon(\omega)$ of this material from reflectance and transmittance measurements of thin films using a Fresnel approach [14]. TDBC was chosen because of its tendency to form J-aggregates: this leads to a narrowing of the optical resonance, making them interesting for strong coupling [15, 16, 17]. More importantly in the present context, at sufficiently high concentrations materials doped with such molecules exhibit a negative permittivity; it is this negative permittivity that enables these materials to support localized resonances. In our previous work [12] a two-oscillator Lorentz model [18, 19] was used to calculate the electric field enhancement and field confinement around the nanoparticle supporting the resonance by use of Mie theory [20, 21]. The field enhancement and confinement we predicted compared favorably with respect to gold nanospheres, albeit over a much narrower spectral range. Here we extend that earlier work by going beyond a simple classical Lorentz oscillator model. In doing so, we are able to explore new transient phenomena and develop a richer microscopic physical picture for the system.

In what follows we first outline the elements and assumptions of the quantum model we have used. We then compute the relative permittivity, $\varepsilon(\omega)$, using this model and compare our results with those obtained from a classical model. We next use our model to investigate the steady-state response of nanospheres of possessing this relative permittivity, with a focus on the nature of the LSEP mode. The response of the same

particle to a suddenly turned on applied optical field is then explored, and the occurrence of transient LSEP modes discussed.

2. Theory

The key difference between the work we report here and previous work based on a bulk, macroscopic approach [12] is that here we develop an effective medium description from a quantum model of the relative permittivity $\varepsilon = 1+\chi$, where χ is the susceptibility. To do so we assume that the molecules in our material can be represented as an ensemble of two-level quantum systems. For a general material, an applied electric field $\boldsymbol{E}$ induces a polarization in the material $\boldsymbol{P} \propto \langle \boldsymbol{d} \rangle$, where $\langle \boldsymbol{d} \rangle$ is the average dipole moment of each molecule (quantum system). Assuming linearity, $\boldsymbol{P}$ is a linear function [22] of $\boldsymbol{E}$, given by:

$$\boldsymbol{P} = \frac{1}{2}\varepsilon_0 \boldsymbol{E}(\chi e^{-i\omega t} + \chi^* e^{i\omega t}) = N\langle \boldsymbol{d} \rangle \tag{1}$$

where N is the number density of quantum emitters, and $\boldsymbol{E}$ and $\boldsymbol{d}$ are generally time and frequency dependent. To find χ and hence ε we need to find $\langle \boldsymbol{d} \rangle$. If we adopt a quantum picture, then $\langle \boldsymbol{d} \rangle$ becomes the expectation value of the dipole moment and can be computed from the trace of $\rho \boldsymbol{d}$, where ρ is the density matrix of the system and $\boldsymbol{d}$ is the dipole moment of each (identical) quantum system (molecule). The density operator $\hat{\rho}$ is defined as $\hat{\rho} = \sum_k p_k |k\rangle\langle k|$, where p_k are the relative probabilities of finding a system element in state $|k\rangle$. In order to find ρ, a Hamiltonian that ~~which can be used to~~ describes the system must be determined. In general, the Hamiltonian for an open quantum system can be expressed as [23, 24],

$$\hat{H} = \hat{H}_0 + \hat{H}_B + \hat{H}_I, \tag{2}$$

where $\hat{H}_0$ is the Hamiltonian of the isolated system, $\hat{H}_B$ describes the interaction of $\hat{H}_0$ with the bath ~~is the bath Hamiltonian which interacts with $\hat{H}_0$~~, and $\hat{H}_I$ ~~is the interaction Hamiltonian to~~ describes the interaction of $\hat{H}_0$ with the applied electric field.

For TDBC molecules in a PVA host medium, $\hat{H}_B$ should represent the $3n_m - 6 = 129$ intramolecular [25] vibrational modes (where n_m is the number of atoms *per* molecule) with a multitude (taken to be an infinite number) of intermolecular modes. These vibrational modes are responsible for induced decay and dephasing in the system [26, 27], along with a small shift in the excited state energy of the molecules [28]. Rather than determine $\hat{H}_B$ directly we have made a commonly-used simplification, that of incorporating the effects of the bath (vibrationally induced decay and dephasing) ~~These effects can be accounted for~~ phenomenologically by application of the dissipative Lindblad superoperator (see below) and by making the assumption that the small energy shift can be ignored ~~By adopting this Lindblad approach, explicit treatment of $\hat{H}_B$ is not~~

~~needed~~ [23, 24].

For an ensemble of n two-level emitters (molecules), $\hat{H}_0$ can be written as [29, 28, 30],

$$\hat{H}_0 = \hbar\omega_0|0\rangle\langle 0| + \sum_{i=1}^{n}\left(\hbar\omega_1^{(1)}|1_i\rangle\langle 1_i| + \sum_{\substack{j=1\\ j\neq i}}^{n} J_{ij}|1_i\rangle\langle 1_j|\right), \tag{3}$$

where $|0\rangle$ is the ground state of the nanoparticle, and $|1_i\rangle$ represents a single exciton excited in the nanoparticle, localized on molecule i, with the other molecules in their ground states *i.e.* $|1_i\rangle = |0_1, ..., 1_i, ...0_n\rangle$. In this way, only a single exciton is permitted within the ensemble at any time. The first term in brackets in Equation (3), $\hbar\omega_1^{(1)}$, represents the average energy eigenvalue of a non-interacting molecule in the excited state (an exciton). The second term corresponds to inter-molecular coupling, with coupling energy J_{ij}. The coupling is taken to be Förster (dipole-dipole) coupling [31, 29] since we assume that the overlap between the wave functions of each site are small. The corresponding interaction Hamiltonian $\hat{H}_I$ modeled in the Schrödinger picture [32] and written in the same basis is,

$$\hat{H}_I = \sum_{i=1}^{n}\left(g_i^*|0\rangle\langle 1_i| + g_i|1_i\rangle\langle 0|\right), \tag{4}$$

where the coupling strength of the dipole to the external optical driving field is defined as $g_i = -\boldsymbol{E}(\boldsymbol{r}_i)\cdot\vec{\mu}_i$, where $\vec{\mu}_i$ is the exciton dipole moment.

Although thorough, a density matrix formed using Equations (3) & (4) would have dimension $(n+1)\times(n+1)$, where n is the number of molecules in the system. Given that n can be several thousand for even a moderately-doped 100 nm diameter nanosphere, solving for such a large matrix would be computationally ~~intractable~~ very demanding, despite considering only a single exciton in the ensemble. We therefore seek a simpler Hamiltonian for a TDBC-doped nanosphere which approximates the formalism above.

As a first step in this process, we identify that for an ensemble of aggregates (where the monomers within each aggregate are aligned with each other), the intra-aggregate coupling terms dominate [33]. This enables us to neglect the inter-aggregate coupling terms. By making this approximation, our approach to describe a nanoparticle doped with randomly distributed and randomly oriented aggregates is to first describe a Hamiltonian for a single aggregate, and then to take an orientational average. ~~This approach significantly eases calculation.~~

The next step is to ~~identify~~ note that for a single aggregate, nearest-neighbour couplings dominate. The Hamiltonian matrix ~~formed~~ obtained under this approximation using

Equation (3) for a single aggregate containing n monomers is,

$$H = \begin{pmatrix} \hbar\omega_0 & 0 & 0 & 0 & \cdots & 0 \\ 0 & \hbar\omega_1^{(1)} & J & 0 & \cdots & 0 \\ 0 & J & \hbar\omega_1^{(1)} & J & \cdots & 0 \\ 0 & 0 & J & \hbar\omega_1^{(1)} & \cdots & 0 \\ \vdots & \vdots & \vdots & \vdots & \ddots & \vdots \\ 0 & 0 & 0 & 0 & \cdots & \hbar\omega_1^{(1)} \end{pmatrix}, \tag{5}$$

where J is the nearest-neighbour interaction energy.The eigenvalues and eigenstates for this Hamiltonian matrix are derived in our Supporting Information `[I SEE EIGENSTATES IN THE SI, EG. EQN S19, BUT I DON'T SEE EIGENVALUES (SEE ALSO COMMENT JEST AFTER EQN 9 BELOW)]`. The first eigenstate is the ground state $|0\rangle$, with energy eigenvalue $\hbar\omega_0$. The second is a set of excited states where a single exciton is delocalized over the aggregate [34, 35],

$$|m\rangle = \sqrt{\frac{2}{n+1}} \sum_{j=1}^{n} \sin\left(\frac{j+1}{n+1} m\pi\right) |1_j\rangle, \tag{6}$$

where $1 < m < n$. The single exciton transition dipole moment of the aggregate $\boldsymbol{d}_{01}(m)$ for mode m is related to the transition dipole moment of the monomers $\vec{\mu}_{01}$ (assuming identical dipole moments) by [36],

$$\boldsymbol{d}_{01}(m) = \vec{\mu}_{01} \sqrt{\frac{1-(-1)^m}{n+1}} \cot\left(\frac{\pi m}{2(n+1)}\right). \tag{7}$$

This implies that $\boldsymbol{d}_{01}(m)$ is zero for even values of m ~~and that $\boldsymbol{d}_{01}(1)/\boldsymbol{d}_{01}(3)$ lies in the vicinity of 3 for $n > 6$. Given that~~. Even for very modest aggregates, $n > 6$, the leading eigenstate ($|1\rangle$) gives rise to a transition dipole moment a factor of three stronger than the next eigenstate, i.e. the leading eigenstate is the 'brightest' `[MARTIN - we need to add an extra reference here, Phys Rev A, vol 53, p2711, 1996]`, we can take the transition dipole moment of the aggregate as $\boldsymbol{d}_{01} = \boldsymbol{d}(1)$, and use the two states $|0\rangle$ and $|1\rangle$ ~~to~~ as an approximation the ~~system~~ aggregate, where $|1\rangle$, using equation 6, is given by,

$$|1\rangle = \sqrt{\frac{2}{n+1}} \sum_{j=1}^{n} \sin\left(\frac{j+1}{n+1}\pi\right) |1_j\rangle. \tag{8}$$

The eigenvalue of $|1\rangle$ is,

$$\hbar\omega_1 = \hbar\omega_1^{(1)} - 2J\cos\left(\frac{\pi}{n+1}\right). \tag{9}$$

`*** WHERE DOES THIS COME FROM ?????  ***`

This allows us to write $\hbar\omega_1 = \hbar\omega_1^{(1)} + \Delta$. The excitation energy of the aggregate is shifted from the monomer value by Δ, and this shift arises from the interaction with other molecules in the aggregate. This energy shift has been observed elsewhere for

aggregates [37, 28], and is loosely termed the 'effect of aggregation' [31]. The magnitude of Δ is typically hundreds of meV [29]. Therefore, by considering ~~these two states only~~ only the ground state and this (brightest) excited state, Equation (3) can be re-written as,

$$\begin{aligned}\hat{H}_0 &\approx \hbar\omega_0|0\rangle\langle 0| + (\hbar\omega_1^{(1)} + \Delta)|1\rangle\langle 1| \\ &= \hbar\omega_0|0\rangle\langle 0| + \hbar\omega_1|1\rangle\langle 1|. \end{aligned} \tag{10}$$

The interaction Hamiltonian for the aggregate is written as,

$$\hat{H}_I = G(|0\rangle\langle 1| + |1\rangle\langle 0|), \tag{11}$$

where $G = \boldsymbol{E}\cdot\boldsymbol{d}_{01}$ is the coupling strength of the electric field, $\boldsymbol{E}$, to the dipole moment, $\boldsymbol{d}_{01}$, of the aggregate. The Hamiltonian formed by adding Equation (10) & (11) can be applied to an ensemble of randomly-distributed aggregates by taking $G = \boldsymbol{E}\cdot\overline{\boldsymbol{d}}_{01}$, where $\overline{\boldsymbol{d}}_{01} = \boldsymbol{d}_{01}/D$ is the orientational average of the aggregate dipole moments in the system of interest, and D is the dimensionality of the space in which the dipoles are distributed. (This orientational average is derived in our Supporting Information, see section 4.)

Our goal now is to find an effective medium value of ε at time t and at the frequency of illumination, ω. The first step is to note that $\hat{H}_I/|E(t)|$ defines the transition dipole matrix $\boldsymbol{d}$ for the system as a whole `[THERE IS A PROBLEM HERE,` d `WAS PREVIOUSLY DEFINED AS THE DIPOLE MOMENT OF A MOLECULE - SEE EQN 1 !!]`. Given that the density matrix (ρ) can be used to obtain the expectation value of an observable, we seek ρ using the Liouville-von Neumann equation [38],

$$\dot{\rho}(t,\omega) = -\frac{i}{\hbar}[H, \rho(t,\omega)] + L_D\rho(t,\omega). \tag{12}$$

The first term in Equation (12) governs unitary evolution. The Lindblad dissipation superoperator [39, 40] L_D, is used to account for the decay and dephasing effects the bath has on the system. In this work, we assume the electron-phonon coupling to be weak at room temperature and for weak fields, and this enables the Born-Markov approximation upon which this formalism relies [41] to be used. The total dephasing rate of the transition $|0\rangle \leftrightarrow |1\rangle$ is Γ_{01}. This quantity is related to the population decay rate for the $|1\rangle \rightarrow |0\rangle$ decay channel, γ_{01}, and the pure dephasing rate, $\Gamma_{01}^{(d)}$, by [39],

$$\Gamma_{01} = \frac{\gamma_{01}}{2} + \Gamma_{01}^{(d)}. \tag{13}$$

The pure dephasing rate, $\Gamma_{01}^{(d)}$, arises from phase-changing interactions of the excitons with the environment [42], *i.e.* the bath of vibrational modes. A ~~more detailed~~ less approximate approach could be adopted [41] [add ref, New Journal of Physics, 2015, vol 17, p 053040], but assuming a simple rate for $\Gamma_{01}^{(d)}$ is sufficient for our present purposes, that of enabling an illustrative calculation to be carried out. A discussion of the

physical origin of $\Gamma_{01}^{(d)}$ is given in our Supporting Information.

For our two-level system, Equation (12) is used to find 4 coupled differential equations [43], the well-known Optical Bloch Equations [44] (OBEs). Solving these for the applied cosine potential allows us to use the Rotating Wave Approximation (RWA) [45], as detailed in our supporting information. To calculate the permittivity, a value for $\boldsymbol{d}$ is chosen, $\langle \overline{\boldsymbol{d}}_{\mathbf{o1}} \rangle$ can then be evaluated using $\langle \overline{\boldsymbol{d}}_{\mathbf{o1}} \rangle = \mathrm{Tr}(\rho \boldsymbol{d})$. Then, by choosing the forward-propagating electric field, Equation (1) allows us to obtain ε for an ensemble of two-level molecules (number density N, arranged in aggregates and randomly distributed in a medium of background permittivity $\varepsilon = \varepsilon_b$), and in the single-exciton regime), as,

$$\varepsilon(t,\omega) = \varepsilon_b + \frac{2N}{\varepsilon_0} \frac{|\overline{\boldsymbol{d}}_{01}|}{|\boldsymbol{E}|} \rho_{01} e^{i\omega t}. \tag{14}$$

This formula holds for weak fields, as we ~~shall now demonstrate~~ show below.

3. Results and Discussion

For our model we require the following parameters: $\overline{\boldsymbol{d}}_{01}$, $\hbar\omega_1$, γ_{01} and $\Gamma_{01}^{(d)}$. We used our experimental reflectivity and transmittance data (for a 1.46 $wt\%$ TDBC:PVA 70 nm film [12]) to determine that $\hbar\omega_1 = 2.11eV \equiv 588\ nm$. This agrees with the values obtained by van Burgel [46] and Valleau [29] although it is a slight change from our previous work, where we indicated that the transition occurred at 2.10 eV (590 nm), with a (weaker) shoulder transition at 2.03 eV (610 nm). Our revised value follows from an improved Kramers-Kronig analysis of our original data, as outlined in our supporting information.

From photoluminescence measurements [47], we took the decay rate of $|1\rangle$ to be $\gamma_{01} = 1.15 \times 10^{12} s^{-1}$ for the aggregate in a PVA host medium. Using Molinspiration ©, we determined the molecular weight and the effective volume of the TDBC molecule. Together with the concentration of the solution, these quantities allowed us to determine the molecular number density to be $N = 1.47 \times 10^{25}\ m^{-3}$. We were then able to estimate the transition dipole moment for TDBC molecules in aggregate form, $\langle \overline{\boldsymbol{d}}_{01} \rangle$, and the dephasing rate, $\Gamma_{01}^{(d)}$, by fitting the steady-state solutions for Equation (14) to our experimental data for $\varepsilon(\omega)$ by adjusting d_{01} and $\Gamma_{01}^{(d)}$. In this way we found the dipole moment to be 48 Debye (D) ~~(corresponding to an effective dipole length of 10.1Å)~~. The TDBC-doped thin films from which the experimental data were obtained were produced by spin-coating [12]. Previous work to investigate the orientation of dipole moments in thin polymer films produced by spin-coating found that the dipole moments lie predominantly in the plane **ADD REF**: Journal of Modern Optics, (2004), 51, p 2287**. Assuming that the TDBC aggregates also lie in the plane of the spun films reported in [12], then the value of 48D we have determined here is a two-dimensionally averaged

value, implying that the on-axis dipole moment of an aggregate is $\boldsymbol{d}_{01}$ 97D, and the three-dimensionally averaged moment is 32D. This three-dimensionally averaged moment compares with the 24D estimated by van Burgel *et al.* [46] from experiments in solution (3-dimensional).

THEN DELETE from ****** to ********

****
This is in line with the value measured by Valleau [29]. Given that our original film was produced by a spin-coat procedure [12, 48], the dimensionality of the orientationally-averaged dipole moment is two. This implies a value for the non orientationally-averaged transition dipole moment of $\boldsymbol{d}_{01} = 97\ D$. This is the value taken by Vasa *et al.* [49], and is consistent with excitons being delocalized over approximately 15 molecular units [46]; aggregate dipole moments are proportional to the square root of the number of molecules in the aggregate [50, 33]. This leads to the monomer value of $\vec{\mu}_{01} = 27\ D$, which is consistent with the 23 D measured by van Burgel [51] and the 27 D calculated by Kelly [52]. The value for $\overline{\boldsymbol{d}}_{01}$ in three dimensions is deduced as 32 D.
****

The dephasing rate, $\Gamma_{01}^{(d)}$, was found to be equal to 17 meV, which is $\approx \kappa_B T$ as expected [29]. To provide additional support for our value of $\Gamma_{01}^{(d)}$, we extracted and modeled $\varepsilon(\omega)$ from the reflectance and transmittance data from a 5.1 nm thick film obtained by Bradley *et al.* [53]. We determined $\Gamma_{01}^{(d)}$ to be around 13 meV, a value comparable with our own, bearing in mind that different bath spectral densities associated with differences in the host and substrate may change the value of $\Gamma_{01}^{(d)}$. Our results for $\varepsilon(\omega)$ against experimentally-determined data for our film are displayed in Figure 1, assuming a planar distribution of dipoles. Also shown is $\varepsilon(\omega)$ for the same concentration, assuming a volume distribution of dipoles. The latter result is mapped onto the former for a concentration of 3.22 $wt\%$, which is the value used from here on out.

3.1. Numerical Results: Steady-State

We now explore theoretically the Mie [20, 21] absorption efficiency spectra $Q_{abs}(\omega)$ for a 100 nm diameter nanosphere of 3.22% TDBC:PVA, assuming a volume distribution of dipole orientations, based on $\varepsilon(\omega)$ calculated using Equation (14). In practice, the applied optical field we model here might be a laser beam. For a 1 mW laser with a spot diameter of 1.5 mm, the strength of the electric field of our incident optical field would be equal to 462 Vm^{-1}; we assume this value here.

In a 100 nm diameter nanosphere of our material, there are on average $n = 1.72{\times}10^4$ molecules. Note that it is the number of molecules and by extension their number den-

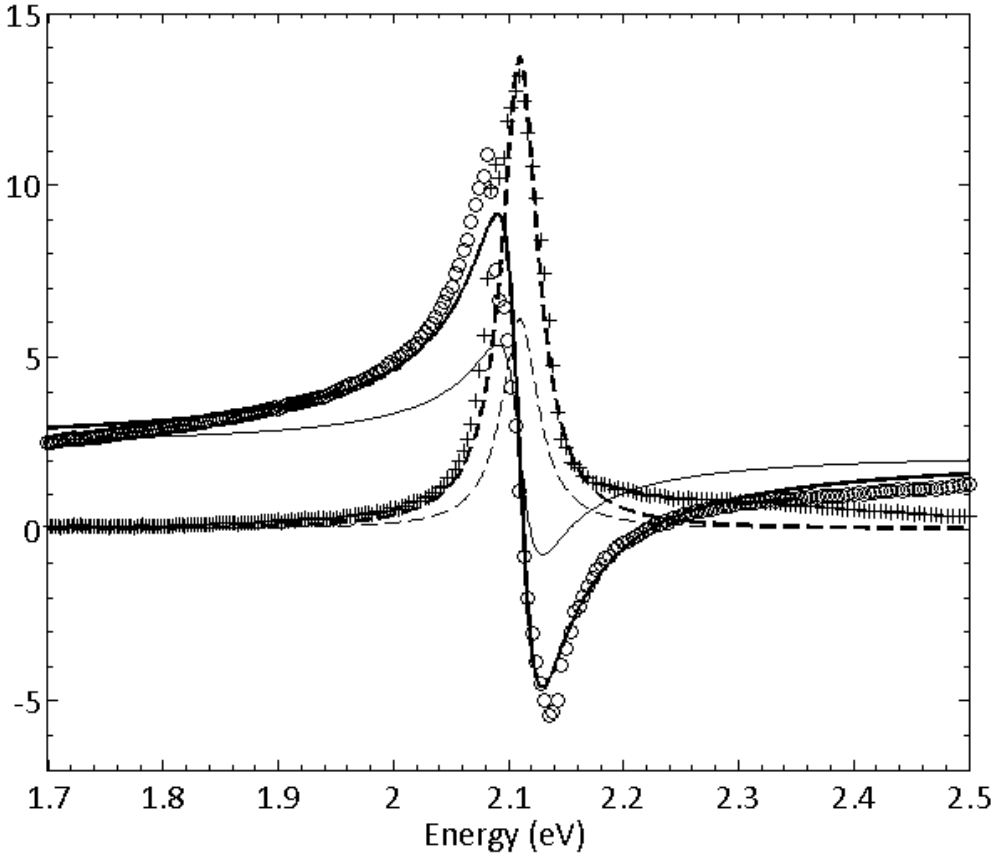

Figure 1. Extracted relative permittivity $\varepsilon(\omega)$ from a 1.46 $wt\%$ TDBC:PVA film (circles for real part and crosses for imaginary part) [12]. $\varepsilon(\omega)$ as determined for this system assuming that the dipoles are distributed in the plane of the film are indicated by the thick solid and dashed lines. The real and imaginary parts of $\varepsilon(\omega)$ for where the dipoles are randomly distributed in three dimensions and for the same concentration are shown by the thin solid and dashed lines.

sity, which is the important quantity (and is used for N in Equation (14)) rather than the number density of aggregates, since each molecule provides a potential site for exciton excitation. To check the validity of our assumption that multi-exciton and nonlinear effects [42] can be neglected, we computed the maximum expectation value of the number of excitons in the nanosphere ($n_{ex} = \max(\rho_{11})n$) using Equations (10) and (11) in Equation (12). We found that $n_{ex}/n \ll 1$ holds for laser powers of up to 10^2 W with a spot size of 1.5 mm. Given that our laser power is 1 mW, we assumed that the single-exciton linear regime is sufficient to describe the system under this illumination power.

In Figure 2 we plot the absorption efficiency $Q_{abs}(\omega)$ for a 100 nm diameter nanosphere, calculated for a variety of permittivities; in each case the absorption efficiency is calculated using Mie theory [20, 21]. Calculated values for Q_{abs} based upon the permittivity

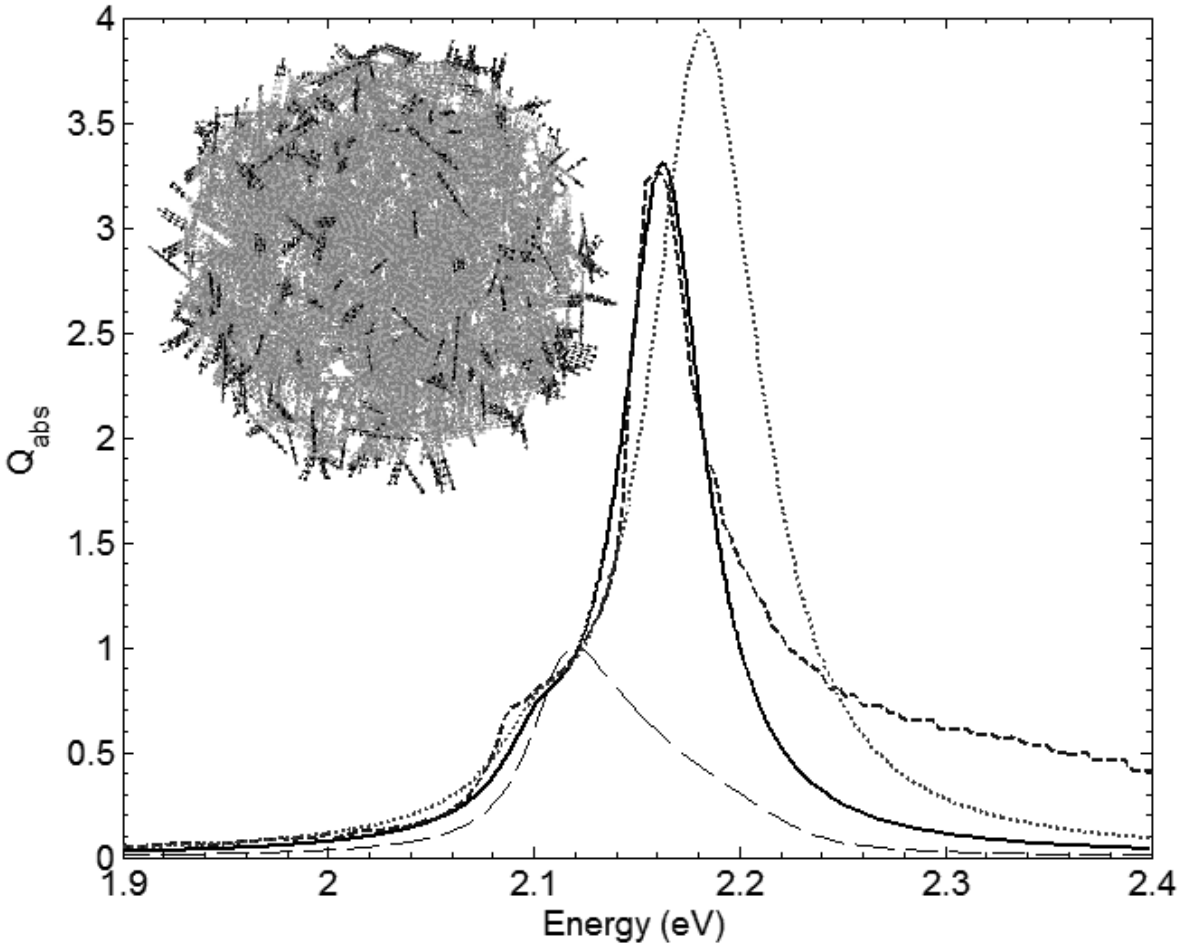

Figure 2. Mie calculations for the absorption efficiency $Q_{abs}(\omega)$ in the steady-state for a 100 nm diameter nanosphere of 3.22 $wt\%$ TDBC:PVA using the values for $\varepsilon(\omega)$ from experiment (dashed line), from two-level OBEs (solid line), and from our previous Lorentz oscillator model (dotted line). The material absorption coefficient κ (imaginary part of the refractive index), normalized to unity, is also plotted for illustrative purposes (long dashed line). Inset: a 3D representation of the aggregated emitters (assuming brick-stone aggregation, with 15 molecules *per* aggregate) randomly distributed in a 100 nm diameter nanosphere.

obtained using our improved analysis of experimental data are shown in Figure 2 as a dashed line. Our quantum theoretical spectrum for Q_{abs}, using $\varepsilon(\omega)$ from Equation (14), is shown as the solid line. This theoretically derived spectrum provides a close match to the extracted data, most importantly for energies in the region of interest below 2.22 eV. For energies exceeding 2.2 eV, there is a limb in the extracted data (dashed curve) which might perhaps be attributed to inhomogeneous (non-Lorentzian) broadening which is not accounted for using the OBEs. Also displayed in Figure 2 is the result for Q_{abs} using a best-fit classical Lorentz oscillator model (the parameters for which can be found in our supporting information) shown as a dotted line. It can be seen that the quantum model outlined in the present paper provides an improved fit to the experimental data. We attribute this to the inclusion of dephasing ($\Gamma_{01}^{(d)}$) in the

model: if $\Gamma_{01}^{(d)}$ were set to zero, a Lorentz model would be recovered in the steady state, and the single damping term in the Lorentz model would have to accommodate both decay and dephasing. Therefore, by including dephasing, the actual physical value of the decay rate γ_{01} can be included to achieve an accurate result for ε.

It is interesting to note a key feature shown by the data in Figure 2: Q_{abs}, reaches its peak value at 2.16 eV (574 nm). This is in contrast to the absorption coefficient, $\kappa(\omega)$, which peaks at 2.12 eV (586 nm), shown as a long dashed line in Figure 2. This difference in spectral position arises because the peak in Q_{abs} is not due simply to absorption: rather, it is due to the excitation of a localized SEP mode [12]. Confirmation of this interpretation comes from two sources. First, in the quasistatic limit the polarizability of the nanosphere follows the Clausius-Mossotti condition, for which resonance occurs when $\varepsilon = -2$ (when the nanosphere is in free space) [54]. From Figure 1 this can be seen to be approximately true for a 100 nm diameter nanosphere, as the permittivity value at the wavelength of peak absorption efficiency, Q_{abs}, is $\varepsilon = -2.251 + 1.728i$. This difference from $\varepsilon = -2$ originates from the fact that $\varepsilon = -2$ only gives the resonance condition if the imaginary part of ε is zero; the complex nature of the permittivity changes the spectral location of the absorption peak. Second, Q_{abs} near the peak goes well above unity: this is associated with field enhancement [2], another signature of a resonant mode. The enhanced electric field in the vicinity of the nanosphere is illustrated graphically in Figure 3(a), together with direction of power flow shown by the Poynting vector $\boldsymbol{S}$.

In Figure 3, the incident electric field is polarized in the x-direction. The Poynting vector arrows shown in the figure were calculated at starting points for which $z = -200$ nm and $x = 0$ nm, linearly spaced in the range -200 $nm \leq y \leq 200$ nm. Subsequent points for evaluation of the Poynting vector were taken at 10 nm steps in the direction of the Poynting vector at each point, resulting in the flux lines shown. The power flow in Figure 3(a) shows that incident light is drawn towards and absorbed by the nanosphere for starting positions up to around 130 nm from the central position of the nanosphere. This demonstrates that at this energy, the nanosphere absorbs more light than the light geometrically striking it [55], and hence $Q_{abs} > 1$. In comparison, absorption at the transition energy, *i.e.* at 2.11 eV is seen only as a shoulder mode in the absorption efficiency of the nanosphere (Figure 2) and the efficiency does not exceed unity. The power flow around the nanosphere for the energy at which κ peaks (2.12 eV) is shown in Figure 3(b), and the enhancement of the field is much weaker than for excitation on resonance at 2.16 eV.

3.2. Numerical Results: Time Domain

We now turn our attention to the time domain. Our theoretical model for dynamic processes in two-level quantum systems subject to a perturbing cosine electric field is

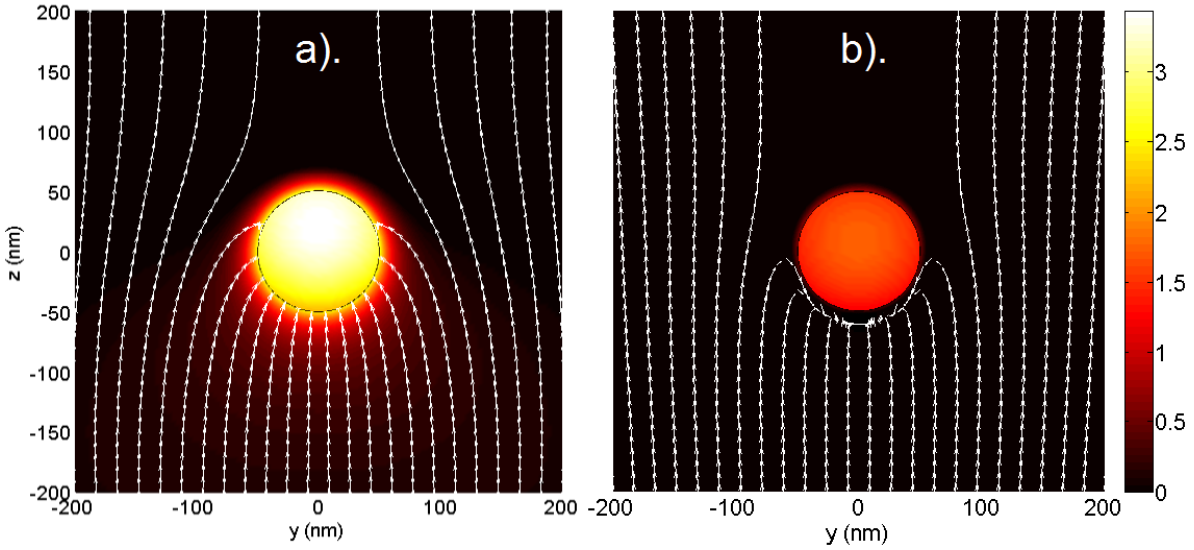

Figure 3. The time-averaged electric field strength normalized to the incident field strength (color plot) and the Poynting vector $\boldsymbol{S}$ (arrows) in the vicinity and on the surface of the 100 nm 3.22 $wt\%$ TDBC:PVA nanosphere, with incident power flow along the positive z-direction. Data are calculated for incident photon energies of a). 2.16 eV = 574 nm and b). 2.12 eV = 586 nm corresponding to peak absorption efficiency and κ respectively.

similar to models considered elsewhere [56, 57, 58, 59], but here the observable of interest arises from the temporal evolution of the coherences of the density matrix, rather than the populations. The dynamics of a two-level ensemble subject to a pulse potential has been the subject of recent investigation [60], but here we investigate a rather different case: that of a cosine potential of fixed amplitude that is switched instantaneously on at some moment in time. We do this to provide an easily soluble model that illustrates the time-dependent phenomena we wish to discuss.

By using Equation (14) to calculate $\varepsilon(t)$ for a given illumination frequency ω as before, $Q_{abs}(t,\omega)$ can be determined and its temporal behavior examined. To do this, we again use Mie theory. This is an approximation since the fields scattered in Mie theory are assumed to be instantaneous. Given that the dynamics seen in Figure 4 evolve over a few femtoseconds and that light propagates over a length scale three times the size of the nanoparticle during a single femtosecond, and that the nanoparticle is illuminated with an electric field of constant amplitude, this approximation is deemed to hold. Mie theory can therefore be used to give a quasi-instantaneous picture of the absorption.

$Q_{abs}(t)$ is shown in Figure 4 for five different detunings, $\delta = \hbar\omega_1 - \hbar\omega$, from the transition at $\hbar\omega_1 = 2.11\ eV$. We assume that all the molecules in the nanoparticle are initially in their ground state. At $t = 0$ we turn on our field abruptly. We see that a steady-state response is attained after $> 200\ fs$, but interestingly, for $\delta = 0.09\ eV$, $Q_{abs}(t)$ repeatedly exceeds unity in spite of the steady-state value of Q_{abs} being below

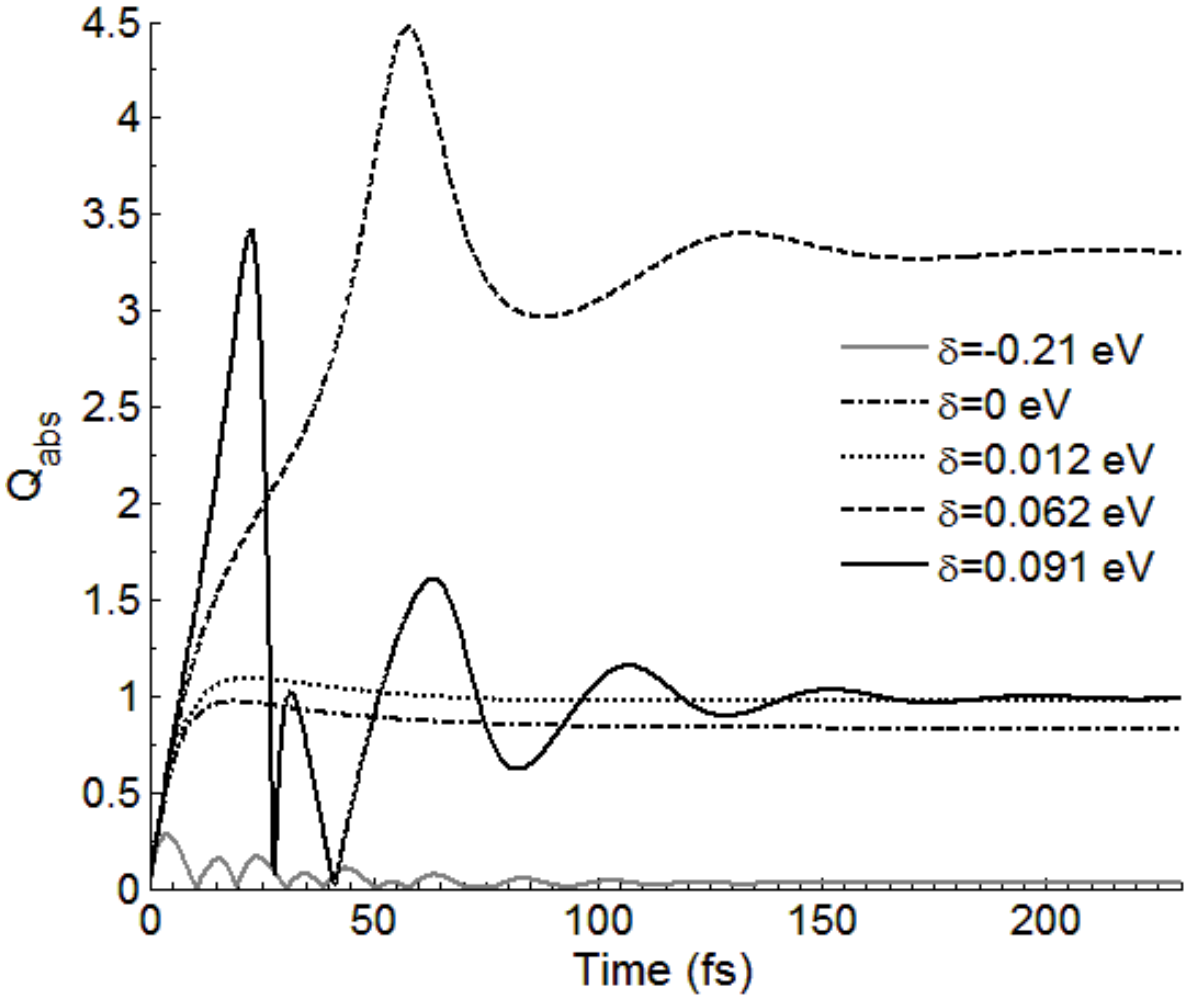

Figure 4. Calculated $Q_{abs}(t,\omega)$ for a 100 nm diameter nanosphere of 3.22% TDBC:PVA warming up a pure state at $t = 0$ with a 1 mW laser set at five different detunings δ from the exciton transition.

unity at this detuning. Since $Q_{abs}(t) > 1$ implies field enhancement, these data are indicative of a transient LSEP mode being present at early times. The time-dependent behavior comprises two contributions: the first is the oscillatory behavior arising from Rabi oscillations; the second is the transient effects associated with the sudden turning-on of the field. In the latter, the magnitude of the density matrix coherences exceed their steady-state values for tens of femtoseconds, resulting in larger values of ε and hence different absorption properties to the steady-state.

If ε passes through the Clausius-Mossotti condition for the nanoparticle as it approaches its steady-state value, Q_{abs} exceeds unity, implying a transient LSEP mode. This is seen best for a detuning of 0.091 eV between $0 - 30$ fs. The Rabi oscillations follow the generalized Rabi frequency $\tilde{\Omega}_R$, given by

$$\tilde{\Omega}_R = \sqrt{\Omega_1^2 + \delta^2}, \tag{15}$$

where, $\Omega_1 \ll \delta$, and $\tilde{\Omega}_R \to \delta$ in this case, Ω_1 and δ are the Rabi frequency and the detuning respectively. These Rabi oscillations are naturally convoluted with the transient effects. This implies, together with the short timescales involved in the system, that it would be a challenge to see these transitory effects, but might perhaps be possible [49]. Critical to the transient LSEP lifetime is $\Gamma_{01}^{(d)}$. If this dephasing could be reduced without losing the transient negative permittivity that is essential for field enhancement (and field confinement), then the transient timescale of the system would be increased up to a maximum of $1/\gamma_{01}$. This corresponds to the picosecond regime for our TDBC:PVA system. Under this circumstance, transient LSEP modes would become more easily observable.

4. Conclusions

We have re-evaluated the measurements reported in our previous work and have obtained an improved permittivity for our J-aggregate-doped 1.46 *wt*% TDBC:PVA polymer film. Using a quantum-mechanical framework we have given support to our previous investigation based on a classical analysis [12], that TDBC doped nanoparticles can exhibit a localized surface exciton-polariton (LSEP) mode. We have used a quantum model to show that these nanoparticles may also exhibit transient LSEP modes in the sub-picosecond regime. These results help strengthen the idea that molecular excitonic materials provide an interesting alternative upon which to base nanophotonics [9]. By using molecular materials the possibility of bottom-up approaches such as supramolecular chemistry and self-assembly can be brought to bear on the production of nanophotonic structures.

Acknowledgments

The work was supported in part by the UK Engineering and Physical Sciences Research Council, and in part by The Leverhulme Trust.

References

[1] Le Ru E C and Etchegoin P G 2009 *Principles of Surface-Enhanced Raman Spectroscopy and related plasmonic effects* 1st ed (Elsevier)
[2] Kreibig U and Vollmer M 1995 *Optical Properties of Metal Clusters* 1st ed (Springer-Verlag)
[3] Kelly K L, Coronado E, Zhao L L and Schatz G C 2003 *J. Phys. Chem. B* **107** 668–677
[4] Stiles P L, Dieringer D J, Shah N C and Van Duyne R 2008 *Ann. Rev. Anal. Chem.* **1** 601–626
[5] Willets K A and Van Duyne R P 2007 *Annu. Rev. Phys. Chem.* **58** 267–97
[6] Taylor R W, Benz F, Sigle D O, Bowman R W, Bao P, Roth J S, Heath G R, Evans S D and Baumberg J J 2014 *Scientific Reports* **4** 1–6
[7] Kitson S C, Barnes W L and Sambles J R 1995 *Physical Review B* **52** 11441–11446
[8] Isaac T H, Barnes W L and Hendry E 2008 *Applied Physics Letters* **93** 2008–2010
[9] Saikin S K, Eisfeld A, Valleau S and Aspuru-Guzik A 2013 *Nanophotonics* **2** 17 (*Preprint* `1304.0124`)

[10] Philpott M R, Brillante A, Pockrand I and Swalen J D 1979 *Mol. Cryst. Liq. Cryst.* **50** 139–162
[11] Lei Gu, Livenere J, Zhu G, Narimanov E E and Noginov M A 2013 *Appl. Phys. Lett.* **103** 021104
[12] Gentile M G, Nunez-Sanchez S and Barnes W L 2014 *Nano Lett.* **14** 2339–2344
[13] Triolo C, Cacciola A, Stefano O D, Genco A, Mazzeo M, Patanè S, Saija R and Savasta S 2015 *ACS Photonics* **2** 971–979
[14] Azzam R M A and Bashara N M 1977 *Ellipsometry and polarized light* 1st ed (North-Holland)
[15] Lidzey D G, Bradley D D C, Armitage A, Walker S and Skolnick M S 2000 *Science* **288** 1620–1623
[16] Dintinger J, Klein S, Bustos F, Barnes W L and Ebbesen T W 2005 *Physical Review B* **71** 035424
[17] Törmä P and Barnes W L 2015 *Reports on Progress in Physics* **78** 013901
[18] Fox M 2010 *Optical Properties of Solids* 2nd ed (Oxford: Oxford University Press) ISBN 978-0-19-957336-3
[19] Lebedev V S and Medvedev A S 2012 *Quant. Electron.* **42**(8) 701–713
[20] Mie G 1908 *Ann. Phys. (Berlin)* **25** 377–445
[21] Bohren C F and Huffman D R 1983 *Absorption and Scattering of Light by Small Particles* (Pennsylvania State University: Wiley)
[22] Mandel L and Wolf E 1995 *Optical Coherence and Quantum Optics* (Cambridge: Cambridge University Press)
[23] Skinner J L and Hsu D 1986 *J. Phys. Chem.* **90** 4931–4938
[24] Abramavicius D, Butkus V and Valkunas L 2011 Interplay of exciton coherence and dissipation in molecular aggregates *Quantum Efficiency in Complex Systems, Part II: From Molecular Aggregates to Organic Solar Cells* (*Semiconductor and Semimetals* vol 85) ed Wurfel U, Thorwart M and Weber E (London: Elsevier) chap 1, pp 3–45
[25] Harris D C and Bertolucci M D 1989 *Symmetry and Spectroscopy: an Introduction to Vibrational and Electronic Spectroscopy* (New York: Dover Publications)
[26] E D, McCumber and Sturge M D 1963 *J. Appl. Phys.* **34** 1682
[27] Harris C B 1977 *J. Chem. Phys.* **67** 5607
[28] Ambrosek D, Khn A, Schulze J and Khn O 2012 *The Journal of Physical Chemistry A* **116** 11451–11458 pMID: 22946964
[29] Valleau S, Saikin S K, Yung M H and Guzik A A 2012 *J. Chem. Phys.* **137** 034109
[30] Spano F C 2012 Vibronic coupling in j-aggregates *J-Aggregates* vol 2 ed Kobayashi T (London: World Scientific) chap 2, pp 49–75
[31] Zhao Y S 2015 *Organic Nanophotonics* (Berlin: Springer)
[32] Parker S P 1993 *McGraw-Hill Encyclopaedia of Physics* (New York: McGraw-Hill Companies)
[33] Knoester J 2002 Optical properties of molecular aggregates *Proceedings of the International School of Physics: Enrico Fermi, Course CLIX* vol 149 (IOS Press) pp 149–186
[34] Malyshev V and Moreno P 1995 *Phys. Rev. B* **51** 14587–14593
[35] Miura Y F and Ikegami K 2012 J-aggregates in the langmuir and langmuir-blodgett films of merocyanine dyes *J-Aggregates* vol 2 ed Kobayashi T (London: World Scientific) chap 14, pp 443–514
[36] Hochstrasser R M and Whiteman J D 1972 *J. Chem. Phys.* **56** 5945–5958
[37] Kuhn H and Kuhn C 1996 Chromophore coupling effects *J-Aggregates* ed Kobayashi T (London: World Scientific) chap 1, pp 1–40
[38] Blum K 1996 *Density matrix theory and application* 2nd ed (New York: Plenum Press)
[39] Schirmer S G and Solomon A I 2004 *Phys. Rev. A* **70** 022107
[40] Breuer H P and Petruccione F 2002 *The Theory of Open Quantum Systems* (New York: Oxford University Press)
[41] Schaller G and Brandes T 2008 *Phys. Rev. A* **78**(2) 022106
[42] Wang K and Chu S I 1987 *J. Chem. Phys.* **86**(6) 3225–3238
[43] Kavanaugh T C and Silbey R J 1993 *J. Chem. Phys.* **98**(12) 9444–9454
[44] Allen L and Eberly J H 1975 *Optical Resonance and Two-Level Atoms* (New York: Wiley)
[45] Dorfman K E, Jha P K, Voronine D V, Genevet P, Capasso F and Scully M O 2013 *Phys. Rev.*

Lett. **111** 043601
[46] van Burgel M, Wiersma D A and Duppen K 1995 *The Journal of Chemical Physics* **102** 20–33
[47] Wang S, Chervy T, George J, Hutchison J A and Genet C 2014 *J. Phys. Chem. Lett.* **5** 1433–1439
[48] Cho J, Char K, Hong J D and Lee K B 2001 *Advanced Materials* **13** 1076–1078
[49] Vasa P, Wang W, Pomraenke R, Lammers M, Maiuri M, Manzoni C, Cerullo G and Lienau C 2013 *Nature Photonics* **7** 128–132
[50] Spano F C, Kuklinski J R and Mukamel S 1990 *Phys. Rev. Lett.* **65**(2) 211–214
[51] van Burgel M 1999 *No Title* Ph.D. thesis University of Groningen
[52] Kelley A M 2007 *Nano Lett.* **7** 3235–3240
[53] Bradley M S, Tischler J R and Bulović V 2005 *Adv. Mater.* **17** 1881–1886
[54] Novotny L and Hecht B 2006 *Principles of Nano-Optics* 1st ed (Cambridge University Press)
[55] Bohren C F 1983 *Am. J. Phys.* **51** 323–327
[56] Fox M 2010 *Quantum Optics An Introduction* (University of Sheffield: Oxford University Press)
[57] Foot C J 2011 *Atomic Physics* (Oxford: Oxford University Press)
[58] Slowik K, Filter R, Straubel J, , Lederer F and Rockstuhl C 2013 *Phys. Rev. B* **88** 195414
[59] Noh H R and Jhe W 2010 *Opt Commun* **283** 2353–2355
[60] Sukharev M, Seideman T, Gordon R J, Salomon A and Prior Y 2014 *ACS Nano* **8**(1) 807–817